International Research Journal on Advanced Engineering Hub (IRJAEH)
e ISSN: 2584-2137
Vol. 04 Issue: 06 June 2026
Page No: 4155 - 4164
https://irjaeh.com
https://doi.org/10.47392/IRJAEH.2026.0537

A Hardware-Secured Wearable Device for Direct Hydration and Vital Monitoring Using Multimodal Sensor Fusion

Mabasha Shaik[1], Dhanush Akkaladevi[2], Vishnu Gosikonda[3], K Harini[4], Bhavani Myaka[5]
[1,2,3,4,5]Department of Computer Science & Engineering (AIML & IoT) Vallurupalli Nageswara Rao Vignana Jyothi Institute of Engineering & Technology, Hyderabad-500090, Telangana, India.
Emails: *mabashapec@gmail.com[1], akkaladevidhanush555@gmail.com[2], vishnu.gk1205@gmail.com[3], kharini1606@gmail.com[4], bhavanimyaka22@gmail.com[5]*

Abstract
Dehydration significantly affects physiological stability, cognitive performance, and overall health. Conventional hydration assess-ment methods are invasive and unsuitable for continuous monitoring. This work proposes a hardware-secured wearable system for real-time hydration and vital monitoring using multimodal sensor fusion and AI-driven analysis. The system integrates bio-impedance analysis (BIA), photoplethysmography (PPG), heart rate, and temperature sensors with an ESP32 microcontroller. A multi-stage inference pipeline performs signal quality assessment, trust estimation, contradiction detection, bio-impedance correc-tion, and temporal hydration prediction using CNN and BiLSTM-based architectures. The framework also incorporates determin-istic risk scoring, uncertainty calibration, and graceful degradation during sensor failure. Experimental evaluation demonstrates reliable hydration trend estimation and stable monitoring under noisy and degraded conditions. The proposed system provides real-time hydration risk assessment and continuous physiological monitoring suitable for healthcare, sports, and wellness applications.
Keywords: *Bio-impedance analysis (BIA); Deep learning; Edge AI; Hydration monitoring; Wearable devices.*

1. Introduction
Dehydration is a largely neglected public health problem in India, heavily influenced by a hot climate and high incidences of gastrointestinal diseases. These environmental and health factors disproportionately affect vulnerable populations such as children and the elderly, leading to serious physiological con-sequences (Figure 1) [1-10].

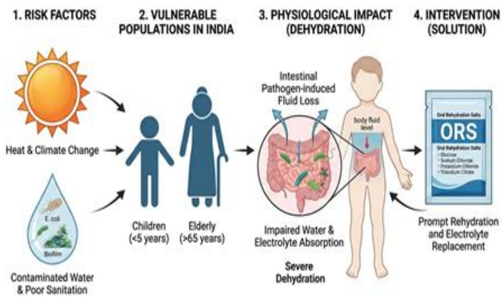

Figure 1 Conceptual Framework Illustrating Dehydration Risk Factors, Affected Populations, And Intervention Strategies

Inadequate water intake and diarrheal diseases remain ma-jor global causes of morbidity Liu et al. (2012, 2015). Clinical studies indicate that up to 70% of pediatric diarrhea cases re-quiring hospitalization associate with severe dehydration. Ef-fective interventions like Oral Rehydration Salts (ORS) exist but remain underutilized. Traditional hydration assessment re-lies on indirect, unreliable methods (subjective thirst, urine color) or invasive laboratory tests, limiting their effectiveness in continuous tracking [11-20].

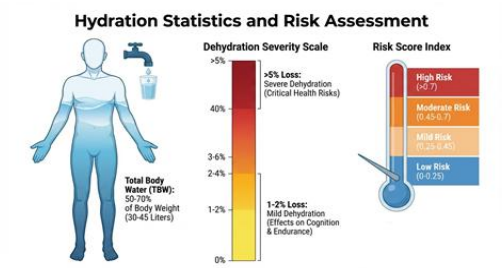

Figure 2 Statistical Representation of Hydration Assessment Based on Total Body Water (TBW)

Total Body Water (TBW) is commonly used to assess hydration, comprising 50-70% of body weight

International Research Journal on Advanced Engineering Hub (IRJAEH)
e ISSN: 2584-2137
Vol. 04 Issue: 06 June 2026
Page No: 4155 - 4164
https://irjaeh.com
https://doi.org/10.47392/IRJAEH.2026.0537

Abdelnour et al. (2024). A 1–2% reduction can cause mild dehydration and cog-nitive impairment, while a >5% loss risks critical complications Adam et al. (2008). Risk scores are classified as low (0–0.25), mild (0.25–0.45), moderate (0.45–0.7), and high (>0.7) to in-terpret hydration-related risks (Figure 2). While isotope dilution is the accurate gold standard for TBW measurement, it is costly. Bioelectrical impedance analysis (BIA) offers a quick, non-invasive, and cost-effective alterna-tive for estimating TBW via electrical conductivity Powers et al. (2009); Lu et al. (2023); Barley et al. (2020). In practice, a ratio of extracellular to total body water >0.39 often reflects fluid overload El Dimassi et al. (2024). The comparison of as-sessment methods is shown in Table 1.

Table 1 Comparison of TBW Assessment Techniques

Method	Accuracy	Cost	Use Case
Isotope Dilution	Very High	High	Clinical trials
BIA / BIS	Moderate -High	Low-Mod	Bedside assessment
DEXA Scan	Moderate	Mod erate	Body composition
Body Weight	High (short-term)	None	Real-time tracking

IoT wearable devices have emerged for continuous data col-lection using sensors like PPG and BIA Andriani et al. (2024); Mirjalali et al. (2022). However, conventional IoT systems pri-marily act as data loggers, lacking the intelligence to interpret complex physiological relationships Rahman et al. (2019). Pure IoT systems struggle with noise, motion artifacts, and missing data, often relying on static thresholds. This work proposes a hardware-secured wearable device in-tegrated with a multi-stage machine learning pipeline for direct hydration and vital monitoring. It incorporates signal quality evaluation, sensor trust modeling, contradiction detection, and deterministic risk assessment to ensure reliable monitoring with improved explainability compared to traditional IoT systems Randazzo et al. (2020); Vo et al. (2024) Shown in Figure 3 - 5.

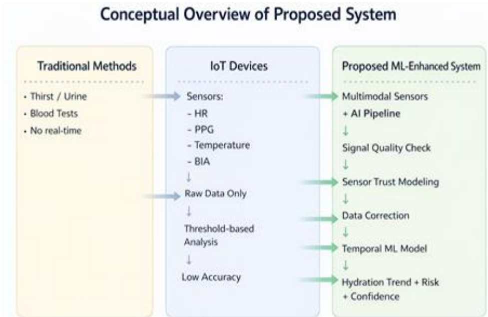

Figure 3 Conceptual Overview of Traditional, IOT-Based, and Ml-Enhanced Hydration Monitoring Systems

2. Method

2.1. Experimental Setup

The experimental setup consists of a wearable hardware pro-totype integrating multiple physiological sensors with an em-bedded microcontroller to acquire, process, and transmit struc-tured data for AI-based hydration analysis.

2.1.1. ESP32 Development Board

The ESP32-WROOM-32 serves as the central controller, supporting ADC inputs and digital communication (I2C/SPI). Operating on a 3.3V power supply, it processes sensor data, formats JSON payloads, and handles Wi-Fi/Bluetooth transmission to the backend API [21-30].

Figure 4 ESP32-WROOM-32 development board RS Components (2024)

Figure 5 ESP32 development board pinout diagram Arduino Forum (2024)

International Research Journal on Advanced Engineering Hub (IRJAEH)
e ISSN: 2584-2137
Vol. 04 Issue: 06 June 2026
Page No: 4155 - 4164
https://irjaeh.com
https://doi.org/10.47392/IRJAEH.2026.0537

2.1.2. Bio-Impedance Analysis Circuit

The BIA System measures body impedance using an AD9833 waveform generator, AD8302 gain/phase detector, and hydrogel electrodes. Passing a safe electrical signal through the body, it outputs an analog voltage representing magnitude and phase. This non-invasive setup is pivotal for hydration estimation but requires stable electrode placement to mitigate motion artifacts Shown in Figure 6 & 7.

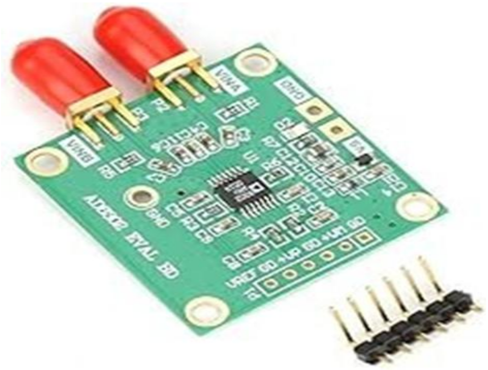

Figure 6 Bio-impedance (Bio-Z) Measurement Sensor

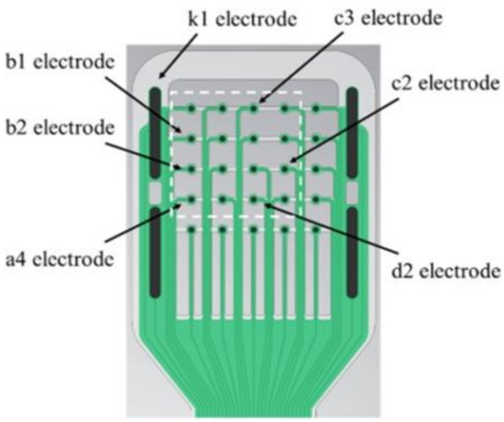

Figure 7 Electrode Configuration for Bio-Impedance Measurement System Kekonen ET Al. (2019)

2.1.3. MAX30102 Pulse Oximeter Sensor

This I2C sensor measures heart rate (HR) and photoplethysmography (PPG) by detecting variations in infrared and red light absorption caused by blood flow. While widely used in wearables, its performance is sensitive to motion and requires proper skin contact. Its high sampling rate supports reliable detection of subtle physiological variations Shown in Figure 8 & 9.

Figure 8 MAX30102 Pulse Oximeter Sensor

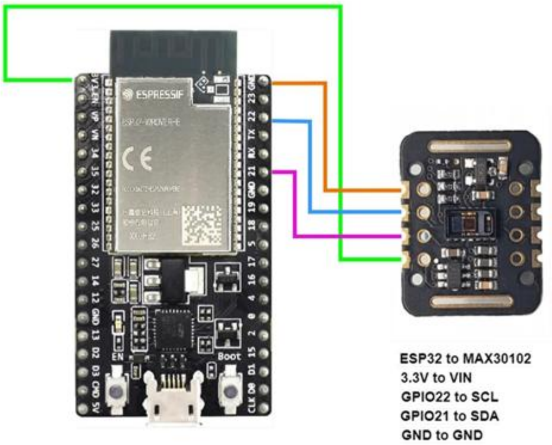

Figure 9 ESP32 and MAX30102 circuit design for pulse oximetry

2.1.4. TMP117 Temperature Sensor

The TMP117 provides accurate peripheral body temperature measurements via the I2C protocol. Internal calibration ensures high-resolution data, essential for correlating metabolic heat with hydration loss [31-35].

2.1.5. MPU6050 (Optional Motion Sensor)

This accelerometer and gyroscope module detects motion artifacts and body movement. By tracking mechanical motion, it enables the AI pipeline to dynamically filter noise from the physiological readings during periods of heavy physical activity Shown in Table 2.

2.1.6. Supporting Components

Breadboards and jumper wires are utilized for rapid prototyping and circuit testing, allowing easy modification of configurations before transitioning to a finalized, compact wearable PCB design Shown in Figure 10 - 13.

International Research Journal on Advanced Engineering Hub (IRJAEH)
e ISSN: 2584-2137
Vol. 04 Issue: 06 June 2026
Page No: 4155 - 4164
https://irjaeh.com
https://doi.org/10.47392/IRJAEH.2026.0537

Figure 10 TMP117 Temperature Sensor

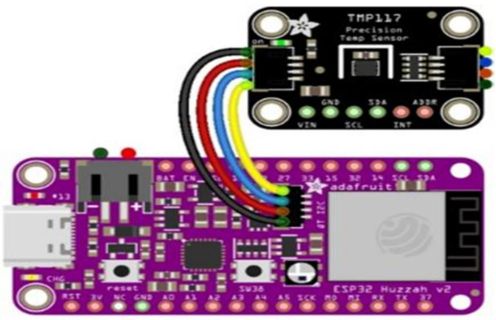

Figure 11 Interfacing TMP117 Temperature Sensor with ESP32 Adafruit (2024)

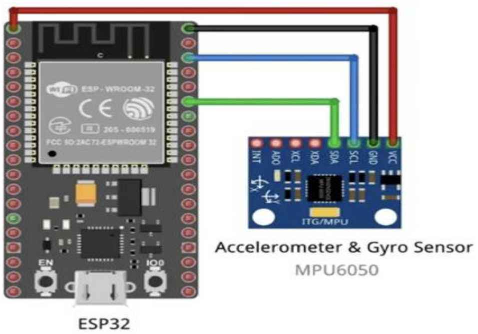

Figure 12 Interfacing MPU6050 with ESP32 via I2C Shilleh (2023)

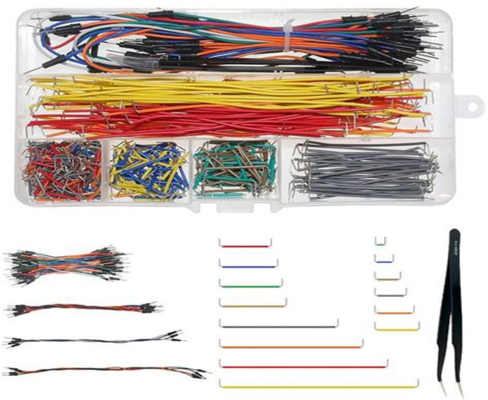

Figure 13 Jumper wires and prototyping components Ubuy (2024)

Table 2 Summary of Hardware Components for the Proposed System

Component	Purpose	Input	Output	Notes
ESP32	Controller	ADC, I2C	Wi-Fi, BT	3.3V Logic
Bio-Imp.	Hydration	Electrical	Analog	AD9833 +AD8302
MAX 30102	HR & PPG	Optical	Digital I2C	Motion sensitive
TMP117	Temp	Thermal	Digital I2C	Accurate sensing
MPU6050	Motion	Mechanical	Digital I2C	Optional sensor

2.2. Dataset Description

To ensure the robustness of the multi-stage AI pipeline, the system utilizes a curated ensemble of datasets spanning bio-impedance, PPG, ECG, and kinematic data. This repository is critical for pre-training models and establishing demographic baselines. All datasets utilized in this study are publicly available and anonymized research datasets obtained from Kaggle, CDC NHANES, and PhysioNet repositories. Preprocessing involved normalization, signal denoising, missing value handling, and temporal segmentation before model training. The datasets were divided into training, validation, and testing subsets to en-sure unbiased performance evaluation.

2.2.1. Wearable Dataset (Stress and Exercise)

Sourced via Kaggle, this dataset provides physiological signals (EDA, HR, Temp, Accel) during induced stress, serving as the training set for Cross-Sensor Contradiction Detection to differentiate artifacts from genuine deterioration.

2.2.2. NHANES Dataset (CDC)

The NHANES dataset offers demographically diverse cross-sectional clinical metrics to establish deterministic thresholds for Risk Scoring, ensuring baseline TBW calculations remain statistically sound Shown in Figure 14 - 15.

International Research Journal on Advanced Engineering Hub (IRJAEH)
e ISSN: 2584-2137
Vol. 04 Issue: 06 June 2026
Page No: 4155 - 4164
https://irjaeh.com
https://doi.org/10.47392/IRJAEH.2026.0537

Table Representation:

Attribute	Description
Dataset Source	Kaggle
Data Type	Multimodal wearable sensor data
Signals Included	HR, EDA, BVP, Temperature, Accelerometer
Format	CSV / Time-series
Number of Subjects	~30–40 participants
Sampling Type	Continuous time-series
Application	Stress detection, wearable analytics
Relevance to Project	Used for training ML models on physiological patterns

Figure 14 Attribute Summary of the Wearable Device Dataset

Table Representation:

Attribute	Description
Dataset Source	CDC NHANES
Data Type	Clinical + physiological + survey
Signals Included	Body measurements, activity, vitals
Format	CSV / SAS files
Number of Subjects	Thousands (large population dataset)
Sampling Type	Cross-sectional
Application	Population health analysis
Relevance to Project	Used for baseline physiological reference

Figure 15 Attribute Summary of the NHANES Dataset

2.2.3. PTB-XL ECG Dataset (PhysioNet)

Comprising over 21,000 ECG recordings, this data pre-trains the temporal attention mechanisms of the Signal Quality Index (SQI) model to robustly identify transient anomalies in cardio-vascular signals Shown in Figure 16.

Table Representation:

Attribute	Description
Dataset Source	PhysioNet
Data Type	ECG signals
Signals Included	12-lead ECG
Format	WFDB / CSV
Number of Records	~21,000
Duration	10 seconds per record
Application	Cardiac analysis, signal processing
Relevance to Project	Used for signal processing and validation

Figure 16 Attribute Summary of the PTB-XL ECG Dataset

2.2.4. Graphen Graphene Bio-Impedance Dataset (PhysioNet)

Containing high-fidelity BIA signals synchronized with blood pressure and PPG, this dataset trains the Bio-Impedance Correction model, providing biophysical constraints to mitigate contact noise and posture drift Shown in Figure 17.

Table Representation:

Attribute	Description
Dataset Source	PhysioNet
Data Type	Bio-impedance + physiological signals
Signals Included	BIA, Blood Pressure, PPG
Format	Time-series
Number of Subjects	~5–10
Sampling Type	Continuous
Application	Hydration & cardiovascular monitoring
Relevance to Project	Core dataset for hydration estimation

Figure 17 Attribute Summary of the Graphene Bio-Impedance Dataset

2.2.5. BIDMC Dataset (PhysioNet)

Featuring synchronized ECG, respiration, and PPG signals from critically ill patients, this dataset provides edge-case scenarios to validate graceful degradation protocols under severe signal attenuation.

2.3. System Architecture and Data Acquisition

The proposed system implements a multi-stage AI pipeline for real-time hydration and vital monitoring. Reliability-aware design ensures robust analysis even during partial sensor failure Shown in Figure 18 - 21.

Table Representation:

Attribute	Description
Dataset Source	PhysioNet
Data Type	Multimodal physiological signals
Signals Included	ECG, Respiration, PPG
Format	WFDB
Number of Subjects	~10–20
Sampling Type	Continuous
Application	Biomedical signal analysis
Relevance to Project	Used for validation and signal modeling

Figure 18 Attribute Summary of the BIDMC Dataset

The architecture spans three layers: Data Acquisition (edge), AI Inference, and Reliability/Fallback. The ESP32 captures and encrypts data via a secure initialization protocol before trans-mission Shown in Table 3.

International Research Journal on Advanced Engineering Hub (IRJAEH)
e ISSN: 2584-2137
Vol. 04 Issue: 06 June 2026
Page No: 4155 - 4164
https://irjaeh.com
https://doi.org/10.47392/IRJAEH.2026.0537

Table 3 Sample Input–Output Mapping of Hydration System

Sample	State	BIA	HR	Temp	SQI	Trend	Risk	Level
1	Healthy	100.23	70.1	37.02	0.95	0.15	0.08	Normal
2	Dehydrating	102.15	72.3	37.15	0.92	0.28	0.32	Mild
3	Severe	112.50	85.2	37.45	0.78	0.85	0.65	Moderate
4	Recovering	110.20	82.5	37.35	0.82	0.60	0.55	Moderate
5	Normalizing	102.50	73.2	37.10	0.90	0.25	0.35	Mild

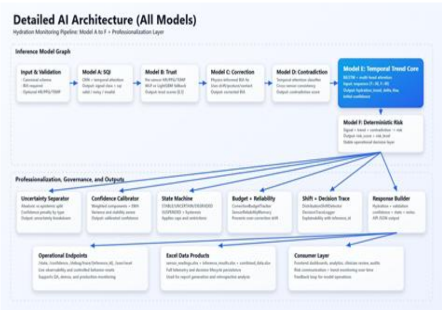

Figure 19 Detailed AI Architecture for Hydration Monitoring System

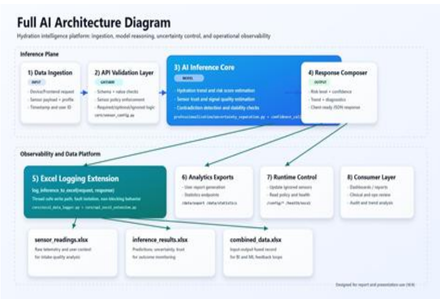

Figure 20 Full AI Architecture Diagram for Hydration Intelligence Platform

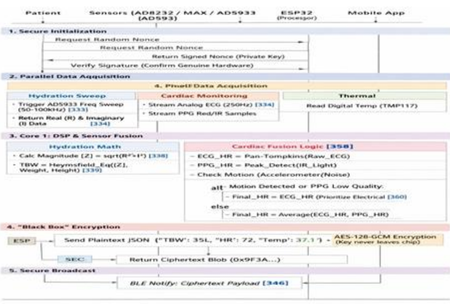

Figure 21 Sequence of Secure Initialization and Data Acquisition

Strict validation protocols govern the system. While BIA is mandatory, auxiliary sensors are handled dynamically. Missing sensors trigger a graceful degradation protocol rather than a system halt (Fig. 23) Shown in Figure 22 - 24.

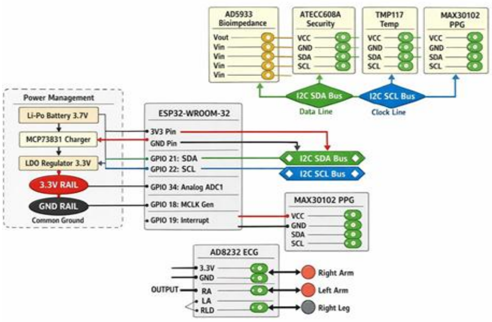

Figure 22 System Schematic: Component Interconnections

Figure 23 Sensor Policy Strategy Categorizing Required and Optional Sensors

2.4. Multimodal Sensor Fusion & AI Pipeline

We employ a dynamic trust-weighted fusion mechanism. Auxiliary sensor inputs $\mathbf{S}_t = [s_{hr,t}, s_{ppg,t},$

International Research Journal on Advanced Engineering Hub (IRJAEH)
e ISSN: 2584-2137
Vol. 04 Issue: 06 June 2026
Page No: 4155 - 4164
https://irjaeh.com
https://doi.org/10.47392/IRJAEH.2026.0537

$s_{temp,t}$] are fused as:

$$\mathbf{F}_t = \mathbf{BIA}_{corr,t} \oplus \sum_{i=1} w_{i,t} \cdot s_{i,t} \qquad (1)$$

The processing core utilizes six distinct models:

- **Model A (SQI):** 1D CNN classifies raw signals as valid/noisy.
- **Model B (Trust Estimation):** MLP assigns trust values to HR/PPG streams.
- **Model C (BIA Correction):** Physics-Informed Neural Net-work (PINN) accounts for posture drift.
- **Model D (Contradiction):** Temporal attention detects inter-sensor physiological disagreements.
- **Model E (Temporal Trend):** BiLSTM network predicts hydration shifts.
- **Model F (Risk Scoring):** Converts outputs into deterministic clinical categories.

2.5. Reliability and Telemetry

The backend uses a FastAPI framework to manage real-time telemetry, separating aleatoric from epistemic uncertainty to govern state machines (STABLE, UNCERTAIN, DE-GRADED). Decision traces are logged for observability. When auxiliary sensors become unavailable due to motion artifacts or communication instability, the framework dynamically adjusts sensor trust weights and continues hydration estimation using remaining valid modalities. This graceful degradation mechanism improves reliability during partial sensor failure.

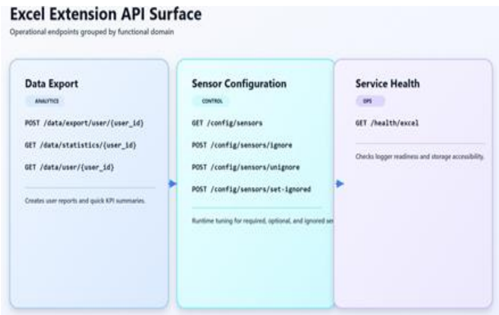

Figure 24 Excel Extension API Surface Showing Data Export Endpoints

3. Results and Discussion

3.1. Results

3.1.1. Core System Performance

Testing across complete and degraded sensor arrays validated the system's adaptability. The AI-driven fusion approach synthesized signals to maintain stable classifications reliably Shown in Table 4 & 5.

Table 4 Core System Performance Metrics and Statistical Summary

Metric	Current Value	Mean Value	Max
Delta TBW (L)	0.4969	0.3010	0.4969
Hydration Trend	0.2313	0.0914	0.2438
Risk Score	0.4564	0.3688	0.4564
Confidence Score	0.6554	0.6650	–
Computed Risk Level MILD (STABLE_ZONE)			

Table 5 Performance Evaluation Metrics of AI Models

Model	Accuracy	Precision	Recall	F1-Score
Signal Quality Model	94.2 %	93.5 %	92.8 %	93.1%
Trust Estimation Model	92.7 %	91.9 %	92.3 %	92.1%
Contradiction Detection	90.8 %	89.7 %	90.1 %	89.9%
Hydration Trend Model	95.1 %	94.8 %	94.5 %	94.6%

3.1.2. Hydration Trend and Risk Calculation

The foundational hydration trend normalizes changes in localized bio-impedance:

$$\text{Trend} = \frac{BIA_t - BIA_{baseline}}{BIA_{baseline}} \qquad (2)$$

The composite risk score is a weighted linear combination of normalized physiological parameters:

$$\textbf{Risk Score} = w_1 \cdot \textbf{Trend} + w_2 \cdot \textbf{HR}_{norm} + w_3 \cdot \textbf{Temp}_{norm} \qquad (3)$$

To prevent false alarms from motion, absolute confidence is dynamically adjusted:

International Research Journal on Advanced Engineering Hub (IRJAEH)
e ISSN: 2584-2137
Vol. 04 Issue: 06 June 2026
Page No: 4155 - 4164
https://irjaeh.com
https://doi.org/10.47392/IRJAEH.2026.0537

$$\textbf{Confidence} = \textbf{Base} \times SQI \qquad (4)$$

Discretized ranges flag states from Normal (0-0.25) to High (>0.70).

3.2. Discussion

3.2.1. Output Diagrams and Benchmarking

The software UI successfully renders detailed metrics (Figure 25), while Figure 26 shows the physical deployment. Compared to pure IoT systems, this architecture delivers improved predictive capability and fault-handling protocols via AI integration (Table 6).

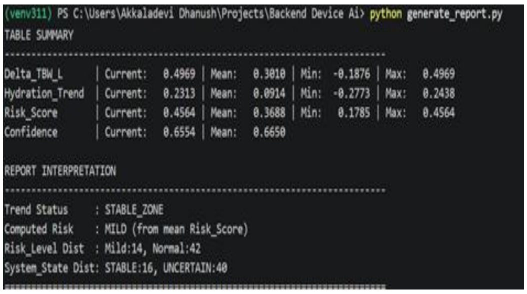

Figure 25 System Output Report Showing Hydration Metrics

Ethical Statement

The study exclusively utilized publicly available anonymized datasets and non-invasive sensing methodologies. No person-ally identifiable information was collected or stored during experimentation.

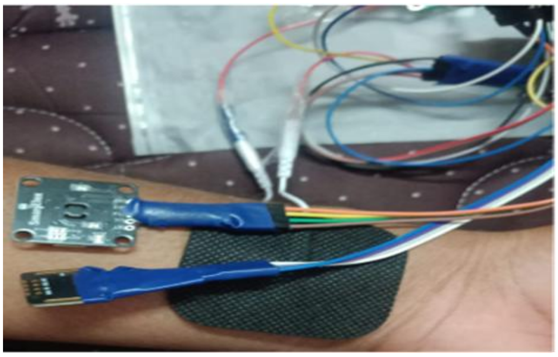

Figure 26 Wearable Prototype with Bio-Impedance Sensor Placement

Table 6 Comparison with Existing IoT Systems

Feature	Pure IoT	Proposed System
Real-time Monitoring	Yes	Yes
AI-based Prediction	No	Yes
Hydration Measurement	Indirect	Direct (BIA)
Accuracy & Reliability	Medium	High
Fault Handling	No	Yes

Conclusion

This work presents a hardware-secured wearable system for real-time hydration and vital sign monitoring using multimodal sensor fusion and AI-driven analysis. By integrating BIA, PPG, heart rate, and temperature sensing, the proposed framework provides continuous hydration assessment with improved reliability compared to conventional IoT-based monitoring systems. The system incorporates signal quality evaluation, trust estimation, contradiction detection, and graceful degradation to maintain operational stability during partial sensor failure. Experimental analysis demonstrates reliable hydration trend estimation and risk prediction under varying physiological conditions. Future work will focus on miniaturized wearable implementation, larger-scale clinical validation, and secure cloud integration for continuous healthcare monitoring.

Acknowledgements

The authors acknowledge the support and facilities provided by Vallurupalli Nageswara Rao Vignana Jyothi Institute of Engineering & Technology for the successful completion of this prototype development.

Competing Interests

The authors declare that they have no competing interests.

Funding

Authors declare they didn't receive any funding in any manner.

References

[1]. Liu, L., Johnson, H. L., Cousens, S., Perin, J., Scott, S., Lawn, J. E., et al. (2012). Global, regional, and national causes of child mortality: an updated systematic analysis for 2010 with time trends since 2000. The Lancet, 379(9832), 2151–2161.

[2]. Liu, L., Oza, S., Hogan, D., Perin, J., Rudan, I., Lawn, J. E., et al. (2015). Global, regional, and national causes of child mortality in 2000–13, with projections to inform post-2015 priorities: an updated systematic analysis. The Lancet, 385(9966), 430–440.

[3]. Abdelnour, M., Berkachy, R., Nasreddine, L., & Fares, E.-J. (2024). Bioelectrical Impedance Vector Analysis (BIVA) for Assessment of Hydration Status: A Comparison between En-durance and Strength University Athletes. Sensors, 24(18), 6024. doi:10.3390/s24186024.

[4]. Adam, G. E., et al. (2008). Hydration effects on cognitive performance during military tasks in temperate and cold environments. Physiology & Behavior, 93(4-5), 748–756.

[5]. Powers, J. S., Choi, L., Bitting, R., Gupta, N., & Buchowski, M. (2009). Rapid measurement of total body water to facilitate clinical decision making in hospitalized elderly patients. The Journals of Gerontology Series A: Biological Sciences and Medical Sciences, 64(6), 664–669. doi:10.1093/gerona/glp018.

[6]. Lu, H., Ayers, E., Patel, P., & Mattoo, T. K. (2023). Body water percentage from childhood to old age. Kidney Research and Clinical Practice, 42(3), 340–348. doi:10.23876/j.krcp.22.062.

[7]. Barley, O. R., Chapman, D. W., & Abbiss, C. R. (2020). Re-viewing the current methods of assessing hydration in athletes. Journal of the International Society of Sports Nutrition, 17(1), 52. doi:10.1186/s12970-020-00381-6.

[8]. El Dimassi, S., Gautier, J., Zalc, V., Boudaoud, S., & Istrate, D. (2024). Body Water Volume Estimation Using Bio Impedance Analysis: Where Are We? IRBM, 45(3), 100839. doi:10.1016/j.irbm.2024.100839.

[9]. Andriani, N., et al. (2024). Monitoring System for Heart Rate and Temperature using MAX30102. International Journal of Scientific Research, 4(2), 56–61.

[10]. Mirjalali, S., et al. (2022). Wearable Sensors for Remote Health Monitoring. Advanced Materials Technologies, 7(1).

[11]. Mireles, C., et al. (2023). Home-care nursing controlled mobile robot with vital signal monitoring. Medical & Biological En-gineering & Computing, 61(2), 399–420.

[12]. Hamad, A. M., & Jasim, A. D. (2021). Remote ECG sig-nal monitoring and classification based on Arduino with AD8232 sensor. University of Thi-Qar Journal for Engineer-ing Sciences, 11(2), 95–101.

[13]. Tao, W., & Jin, Z. (2023). Remote sensing image characteristics and typical area analysis. Sensors, 23(4), 2108.

[14]. Espinosa-Gavira, M. J., et al. (2024). Characterization and per-formance evaluation of ESP32 for real-time synchronized sensor networks. Procedia Computer Science, 237, 261–268.

[15]. Zhang, Y., et al. (2020). Development of a Continuous Blood Pressure Monitoring System. BIODEVICES.

[16]. Kumar, A., & Singh, I. (2025). Arrhythmia Detection using AD8232 ECG Sensor. Preprint.

[17]. Rahman, A., et al. (2019). IoT based patient monitoring system using ECG sensor. ICREST.

[18]. Randazzo, V., et al. (2020). A wearable smart device to monitor multiple vital parameters. Electronics, 9(2), 300.

[19]. Mirjalali, S., et al. (2022). Wearable Sensors for Remote Health Monitoring. Advanced Materials Technologies, 7(1).

[20]. Vo, D.-K., et al. (2024). Advances in wearable biosensors. Biosensors, 14(11), 560.

[21]. Ullah, I., et al. (2024). UVC-Enabled Smart Bandage. Engi-neering Proceedings, 52(1), 12.

[22]. Mata-Romero, M. E., et al. (2024). Low-cost wearable temper-ature device. Sensors, 24(6), 1944.

[23]. Dolson, C. M., et al. (2022). Wearable temperature prediction review. Sensors, 22(19), 7639.

[24]. Volpes, G., et al. (2024). Wearable ring biomedical device. Biosensors, 14(4), 205.

[25]. Clark, K. M., et al. (2023). Wearable sweat

International Research Journal on Advanced Engineering Hub (IRJAEH)
e ISSN: 2584-2137
Vol. 04 Issue: 06 June 2026
Page No: 4155 - 4164
https://irjaeh.com
https://doi.org/10.47392/IRJAEH.2026.0537

sensors. ACS Sen-sors, 8(10), 3606–3622.
[26]. Bertemes-Filho, P. (2021). Wearable bioimpedance devices. Springer.
[27]. Shin, S., et al. (2025). Microfluidic wearable sensor. Science Advances, 11(33).
[28]. Hanze, M., et al. (2025). Textile-based microfluidics. Lab on a Chip, 25(1), 28–40.
[29]. RS Components. (2024). ESP32-WROOM-32 Development Board. Retrieved from https://www.rs-online.com
[30]. Arduino Forum. (2024). ESP32 Pinout. Retrieved from http s://forum.arduino.cc/
[31]. Kekonen, A., et al. (2019). Bioimpedance Sensor Array for Monitoring. Sensors, 19(11), 2505.
[32]. Adafruit. (2024). TMP117 Temperature Sensor Guide. Re-trieved from https://learn.adafruit.com/
[33]. Shilleh. (2023). MPU6050 with ESP32 Setup. Retrieved from https://dev.to/
[34]. Ubuy. (2024). Jumper Wire Kit. Retrieved from https://ww w.ubuy.co.in/
[35]. Espressif Systems. (2024). ESP32 Datasheet. Retrieved from https://www.espressif.com/